

## A terahertz two-wire waveguide with low bending loss

Marx Mbonye, Rajind Mendis, and Daniel M. Mittleman<sup>a)</sup>

Department of Electrical and Computer Engineering, Rice University, MS 366, Houston, Texas 77251-1892, USA

(Received 29 September 2009; accepted 29 October 2009; published online 10 December 2009)

We present experimental and theoretical evidence for low loss terahertz pulse propagation along a two-wire waveguide. We find that the mode pattern at the end of the waveguide resembles that of a dipole, consistent with the fundamental transverse-electromagnetic mode of the structure. Compared to the weakly guided Sommerfeld wave of a single wire, this structure exhibits much lower bending losses. We also observe that a commercial 300  $\Omega$  two-wire TV-antenna cable can be used for guiding frequency components up to  $\sim 0.2$  THz, although they are generally designed to operate only up to about 800 MHz. © 2009 American Institute of Physics. [doi:10.1063/1.3268790]

Over the past decade, tremendous progress has been made in the study of terahertz (THz) waveguides. Single mode coupling and propagation of THz radiation has been demonstrated in a variety of waveguides, including both metallic and dielectric structures.<sup>1-16</sup> In particular, a bare metal wire has attracted a great deal of attention for several reasons, including the simplicity of the design and its connection to plasmonics.<sup>17</sup> Nevertheless, since the primary mode (the Sommerfeld wave) of a single wire is radially polarized, the commonly used linear dipole THz emitter cannot be used for the efficient excitation of this mode, and efficient coupling to a single wire requires the use of circular photoconductive antennas.<sup>9</sup> Moreover, the weakly guiding nature of the Sommerfeld wave leads to high losses when the wire is bent, which limits the practical applications of this waveguide.<sup>7,8</sup>

In this letter, we show that a linearly polarized wave can be efficiently coupled in an end-fire configuration to one end of a two-wire waveguide, if the input polarization is parallel to a line connecting the wire axes. We characterize the fundamental transverse-electromagnetic (TEM) mode of this two-conductor structure by mapping the field pattern at the output, and compare the attenuation to predicted values. Significantly, we find that the bending loss is considerably lower than in the case of a single wire waveguide.

Our experimental setup (inset of Fig. 1) consists of a THz transmitter/receiver pair (fiber coupled photoconductive dipole antennas) and two cylindrical stainless-steel wires that form the waveguide. Each wire is 300  $\mu\text{m}$  in diameter and 24 cm long. The center-to-center wire separation is constant along the length, equal to 0.5 cm. The wires are supported using several slabs of Styrofoam which are nearly transparent to THz radiation. Near the transmitter, the waveguide is bent to an angle of about 45° in order to separate the guided mode from the (uncoupled) wave propagating freely in space. The THz waveform represented by the dashed curve in Fig. 1 is obtained when the two-wire waveguide is in place. The solid curve is obtained when the waveguide is absent, with the THz emitter and receiver undisturbed, indicating no line-of-sight transmission of freely propagating radiation from the emitter to the receiver in this time window.

Next, we image the electric field at the output end of the two-wire waveguide, in a plane perpendicular to the wire axes. The THz receiver (with a 1.5 mm aperture for improved spatial resolution) is raster-scanned in an 8  $\times$  6 mm<sup>2</sup> grid in steps of 1 mm. By orienting the receiver parallel and perpendicular to the center-to-center line, we observe both orthogonal electric field components of the propagating mode. Once these two components are measured, the data sets are combined to obtain the total electric field in magnitude and direction, as shown in Fig. 2. We also show measured THz waveforms at several points along the center-to-center line. Here, we observe a polarity flip for the field between the wires, relative to the field above and below the wires, due to the dipolar nature of the propagating TEM mode.

We also determine the loss characteristics of the waveguide by comparing THz pulses that have propagated through two different lengths, as in previous experiments.<sup>1-4,7,8,13</sup> For both lengths, we use the same 45° bend immediately after the transmitter, which introduces a fixed coupling and bending loss. We change only the length of the straight section, and extract the intrinsic loss on a straight waveguide by normalizing out these effects. The two main pulses [Fig. 3(a)] are almost identical in shape, indicating the negligible group velocity dispersion expected for the fundamental TEM mode. The ringing following the main pulse is repeatable and most likely due to the excitation of

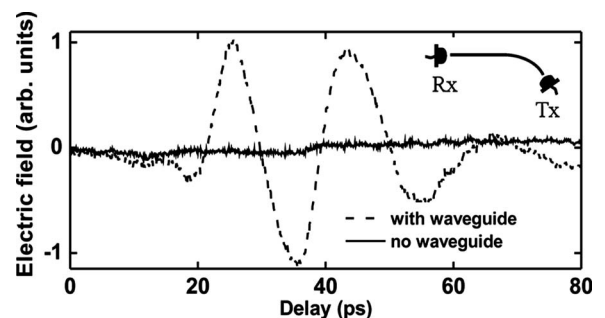


FIG. 1. Dotted line: Transmitted THz pulse along a 24 cm two-wire waveguide, 0.5 cm wire separation. Solid line: measured when the two-wire waveguide is absent with the THz emitter and receiver remaining fixed in position. The inset shows the experimental setup, where the two wires are presented with their center-to-center line perpendicular to the plane of the figure.

<sup>a)</sup>Electronic mail: daniel@rice.edu.

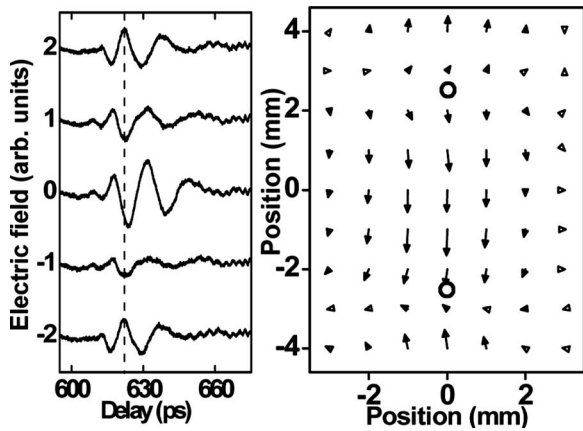


FIG. 2. (Right) The THz receiver is raster scanned around a  $8 \times 6 \text{ mm}^2$  area at the output end of the waveguide. The field mapping is done for both the vertical and horizontal (collection) polarization of the THz receiver while keeping the orientation of the emitter unchanged. The data sets for both polarizations are combined to generate the resultant electric field in magnitude and direction shown by arrows. The circles show the locations of the two wires. (Left) THz waveform for points along the center-to-center line axis of the wires are shown. The waveforms are measured every 2 mm. Note the flip in polarity (along the vertical dashed line) in the upper and lower waveforms compared to the central one. Waveforms vertically offset for clarity.

higher-order modes. The low-loss nature of the propagation is clear from the relatively small change in amplitude. The corresponding amplitude spectra obtained by Fourier transforming the truncated pulses (at the dashed line) are shown in the inset.

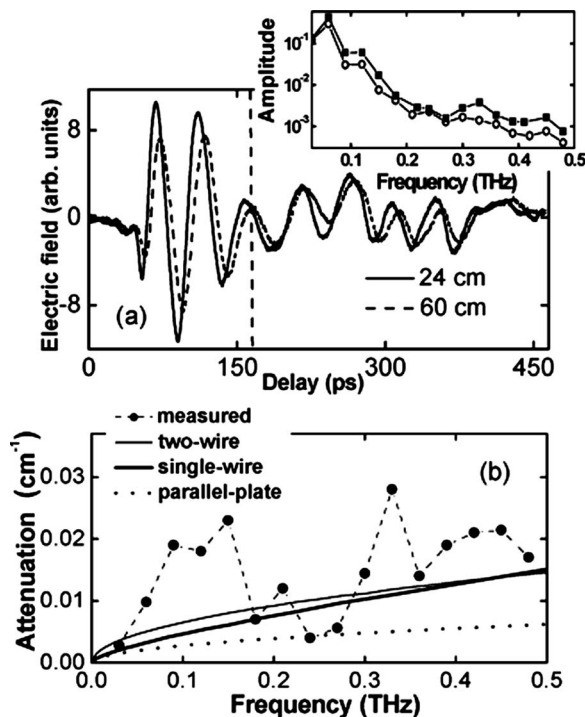


FIG. 3. (a) Transmitted THz pulses along a 60 cm and 24 cm waveguide. The inset shows the spectra for the pulses after truncation at the dashed line. (b) Amplitude attenuation coefficient. Dots: Measured for two-wire waveguide, stainless steel with 0.5 cm wire separation. Thin curve: Calculated values corresponding to the measurement conditions. Thick curve: Calculated values for a single-wire stainless steel waveguide (Sommerfeld wave) of 0.3 mm diameter. Dotted curve: Calculated values for a stainless steel parallel-plate waveguide with 0.5 cm plate separation.

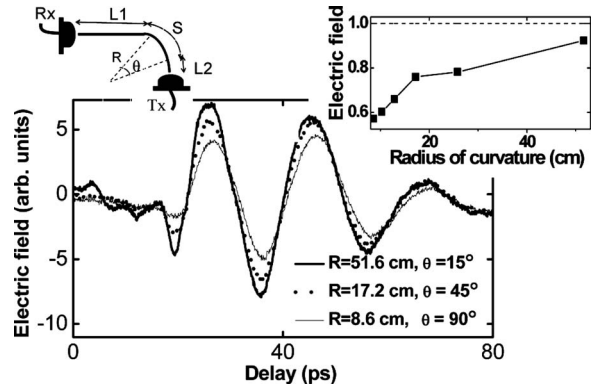


FIG. 4. Transmitted THz pulses along a 65 cm waveguide with various radii of curvature. Solid  $R=51.6 \text{ cm}$  ( $\theta=15^\circ$ ). Dotted line:  $R=17.2 \text{ cm}$  ( $\theta=45^\circ$ ). Thin:  $R=8.6 \text{ cm}$  ( $\theta=90^\circ$ ). The top left inset shows a schematic of the experimental set-up. The top right inset shows the THz peak-to-peak electric field normalized to the value corresponding to no bend ( $\theta=0^\circ$ ).

The (amplitude) attenuation coefficient derived using the measured spectra is shown in Fig. 3(b). For comparison, we also show the computed attenuation for the two-wire waveguide (TEM mode)<sup>18</sup> and for a single-wire waveguide (Sommerfeld wave). The wires in these calculations are assumed to have a diameter of 0.3 mm and a conductivity of  $1.45 \times 10^6 \text{ S/m}$  (type 304 stainless steel), as in our experiments. For comparison, the dotted curve shows the attenuation for the TEM mode of a stainless steel parallel-plate waveguide with a plate separation of 0.5 cm. The measured attenuation of the two-wire waveguide is relatively low and is in reasonable agreement with its theoretical value.

In addition to measuring the attenuation of the two-wire waveguide, we also measure the bending loss. The left inset of Fig. 4 shows a schematic of the setup for a 65 cm long waveguide. The straight section of the waveguide near the receiver is labeled  $L_1$ , the bent section  $S$ , and the straight section near the emitter  $L_2$ . The bend angle is  $\theta$  and the radius of curvature is  $R$ . We keep the receiver fixed, and only vary the bend angle, and the location of the emitter (which is fixed relative to the straight section  $L_2$ ). Since the lengths  $L_1$ ,  $S$ , and  $L_2$  remained the same for every bend angle, any changes in transmission with changing  $\theta$  result only from variations in the bending loss. The time-domain waveforms for several values of  $R$  are shown in Fig. 4. As expected, the signal decreases with increasing bend angle, but the decrease is not rapid. Even with a relatively small radius ( $R=8.6 \text{ cm}$ , corresponding to a  $90^\circ$  bend), there is still a significant THz signal guided to the receiver. This demonstrates the tight coupling of the propagating wave to the two wires, in contrast to the Sommerfeld wave of a single wire where the wave is weakly coupled. For an equivalent bend on a single wire waveguide,<sup>8</sup> the attenuation would be more than a factor of 10, considerably larger than the value measured here which is less than a factor of 2. The right inset shows the peak-to-peak electric field versus bend radius, normalized to the value corresponding to no bend ( $\theta=0^\circ$ ).

Finally, we tested a commercially available 300  $\Omega$ , 18 gauge twin-pair TV antenna cable. This is basically a two-wire waveguide, where the wires are completely enclosed within a dielectric medium (polyethylene), as shown in the inset of Fig. 5(b). Each wire consists of seven copper strands of about 500  $\mu\text{m}$  diameter woven together. The center-to-center separation is about 0.3 cm. The length of the cable

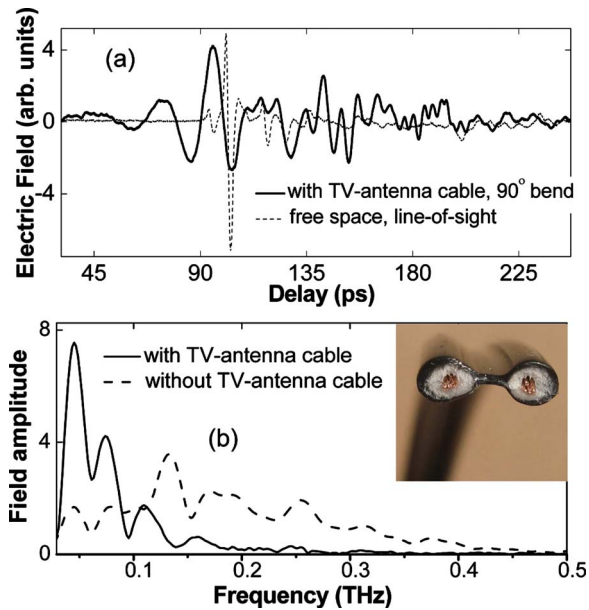


FIG. 5. (Color online) (a) Thick solid curve: THz pulse transmitted through a 9.5 cm length of commercially available TV twin-lead antenna cable, with THz emitter and receiver at  $90^\circ$  to one another. If the cable is removed with the transmitter and receiver in this orientation, no signal is measured. Dashed curve: The free-space THz transmission along a direct line-of-sight between the transmitter and receiver separated by the same 9.5 cm spacing, with no waveguide or optics in between. (b) Amplitude spectra for the two THz waveforms shown in (a). Compared to free-space transmission, the guided wave contains more low-frequency content, which indicates that the twin-lead antenna cable does act as a waveguide, suppressing diffraction losses. Frequencies up to  $\sim 0.2$  THz are guided around the  $90^\circ$  bend. The inset shows a photograph of the antenna cable, showing its cross-section.

used in our measurements is 9.5 cm. We position this length of cable between the THz transmitter and receiver, incorporating a  $90^\circ$  bend so that no freely propagating radiation can be detected. After measuring the propagated signal, the antenna cable is removed, and the measurement is repeated with the emitter and receiver undisturbed. As anticipated, no detectable THz signal is observed in this configuration. Finally, the receiver is repositioned to face the emitter (with the distance between them kept at 9.5 cm), and the measurement is repeated for the freely propagating beam.

The THz waveforms for these measurements are shown in Fig. 5(a). For the signal with the antenna cable (thick solid trace), we observe a positive chirp in the initial burst (up to 110 ps), with high frequency components arriving later in time. This dispersive behavior is distinct from both the free-space wave [dashed curve in Fig. 5(a)] and the TEM mode propagating in the two-wire waveguide (as in Fig. 1), probably because some of the energy propagates in air while some propagates in the polyethylene casing.<sup>19</sup> The long-lived oscillations following the initial burst may be due to the excitation of higher-order modes.

Figure 5(b) gives the spectra corresponding to the two waveforms in Fig. 5(a). We observe greater low-frequency content in the guided signal compared to the freely propagated one. This demonstrates that the antenna cable has functioned as a waveguide, inhibiting the diffractive losses (which are higher at low frequencies), and transporting signals around a  $90^\circ$  bend. The dramatic drop in the high-frequency content is probably due to the additional losses caused by the dielectric medium, which likely represents the dominant loss mechanism. Nonetheless, we find that this TV-antenna cable can carry frequency components up to about 0.2 THz, although these are generally designed to carry frequencies only up to about 800 MHz [ultrahigh-frequency TV broadcast band].<sup>20</sup>

In summary, we have studied the THz propagation characteristics of two-wire waveguides. Experimental results indicate that the mode at the end of the waveguide resemble a dipole pattern, consistent with the fundamental TEM mode of this two-conductor structure. The demonstrated low attenuation and bending loss is consistent with early results at microwave frequencies.<sup>21,22</sup> We also demonstrate that a commercial  $300\ \Omega$  twin-pair TV-antenna cable can be used to propagate radiation up to about 0.2 THz, with large bend angles.

- <sup>1</sup>G. Gallot, S. P. Jamison, R. W. McGowan, and D. Grischkowsky, *J. Opt. Soc. Am. B* **17**, 851 (2000).
- <sup>2</sup>S. P. Jamison, R. W. McGowan, and D. Grischkowsky, *Appl. Phys. Lett.* **76**, 1987 (2000).
- <sup>3</sup>R. Mendis and D. Grischkowsky, *J. Appl. Phys.* **88**, 4449 (2000).
- <sup>4</sup>R. Mendis and D. Grischkowsky, *Opt. Lett.* **26**, 846 (2001).
- <sup>5</sup>H. Han, H. Park, M. Cho, and J. Kim, *Appl. Phys. Lett.* **80**, 2634 (2002).
- <sup>6</sup>K. Wang and D. M. Mittleman, *Nature (London)* **432**, 376 (2004).
- <sup>7</sup>T.-I. Jeon, J. Zhang, and D. Grischkowsky, *Appl. Phys. Lett.* **86**, 161904 (2005).
- <sup>8</sup>K. Wang and D. M. Mittleman, *J. Opt. Soc. Am. B* **22**, 2001 (2005).
- <sup>9</sup>J. A. Deibel, K. Wang, M. D. Escarra, and D. M. Mittleman, *Opt. Express* **14**, 279 (2006).
- <sup>10</sup>B. Bowden, J. A. Harrington, and O. Mitrofanov, *Opt. Lett.* **32**, 2945 (2007).
- <sup>11</sup>M. Skorobogatiy and A. Dupuis, *Appl. Phys. Lett.* **90**, 113514 (2007).
- <sup>12</sup>W. Zhu, A. Agrawal, and A. Nahata, *Opt. Express* **16**, 6216 (2008).
- <sup>13</sup>R. Mendis and D. M. Mittleman, *Opt. Express* **17**, 14839 (2009).
- <sup>14</sup>R. Mendis and D. M. Mittleman, *J. Opt. Soc. Am. B* **26**, A6 (2009).
- <sup>15</sup>S. Atakaramians, S. Afshar, H. Ebendorff-Heidepriem, M. Nagel, B. Fischer, D. Abbott, and T. Monro, *Opt. Express* **17**, 14053 (2009).
- <sup>16</sup>K. Nielsen, H. Rasmussen, A. Adam, P. Planken, O. Bang, and P. Jepsen, *Opt. Express* **17**, 8592 (2009).
- <sup>17</sup>V. Astley, R. Mendis, and D. M. Mittleman, *Appl. Phys. Lett.* **95**, 031104 (2009).
- <sup>18</sup>S. Ramo, J. R. Whinnery, and T. V. Duzer, *Fields and Waves in Communication Electronics* (Wiley, New York, 1965).
- <sup>19</sup>R. Mendis, *Opt. Lett.* **31**, 2643 (2006).
- <sup>20</sup>R. Schneider and J. Ross, *IEEE Spectr.* **46**, 44 (2009).
- <sup>21</sup>K. Tomiyasu, *Proc. IRE* **38**, 679 (1950).
- <sup>22</sup>G. Goubau, *IRE Trans. Microwave Theory Tech.* **4**, 197 (1956).